A Probabilistic Assessment of the Next Geomagnetic Reversal

Bruce Buffett,[1] William Davis[1]

Corresponding author: Bruce Buffett, Department of Earth and Planetary Science, University of California, Berkeley, CA, USA. (bbuffett@berkeley.edu)

[1]Department of Earth and Planetary Science, University of California, Berkeley, CA, 94720-4767 USA.

Deterministic forecasts for the next geomagnetic reversal are not feasible due to large uncertainties in the present-day state of the Earth's core. A more practical approach relies on probabilistic assessments using paleomagnetic observations to characterize the amplitude of fluctuations in the geomagnetic dipole. We use paleomagnetic observations for the past two million years to construct a stochastic model for the axial dipole field and apply well-established methods to evaluate the probability of the next geomagnetic reversal as a function of time. For a present-day axial dipole moment of 7.6×10^{22} A m^2, the probability of the dipole entering a reversed state is less than 2% after 20 kyr. This probability rises to 11% after 50 kyr. An imminent geomagnetic reversal is not supported by paleomagnetic observations. The current rate of decline in the dipole moment is unusual, but within the natural variability predicted by the stochastic model.

1. Introduction

The strength of the geomagnetic dipole has been declining since the first direct measurements were made in 1832 [*Malin*, 1987]. The rate of decline greatly exceeds the rate of decay by diffusion [*Olson*, 2002], prompting speculations that the Earth may be entering the early stage of a geomagnetic reversal [*Hulot et al.*, 2002]. Much of the present-day decline is attributed to transport of magnetic flux from high latitudes toward the equator [*Finlay et al.*, 2016]. However, a rearrangement of magnetic flux exclusively at the core-mantle boundary is probably insufficient to produce a reversal because the axial dipole outside the core reflects the volume-averaged axial magnetic field in the core [*Davidson*, 2001, p. 173]. On the other hand, a synchronous reorganization of the internal magnetic field cannot be ruled out [*Metman et al.*, 2018]. We currently lack sufficient information about the internal configuration of the core to make reliable forecasts using numerical geodynamo models [*Kuang et al.*, 2009; *Aubert and Fournier*, 2011; *Aubert*, 2014]. Forecasts are also affected by fundamental limitations in the predictability of complex dynamical systems [e.g. *Hulot et al.*, 2010].

Paleomagnetic observations offer an alternative way to address the question of the next geomagnetic reversal because records of past behavior can serve as a basis for making inferences about the future. In particular, *Constable and Korte* [2006] found several intervals in the last 7 kyr with rates of dipole decline comparable to the present-day observations. None of these intervals of rapid decline led to a reversal, suggesting that the present trend is simply part of the natural variability of the geomagnetic field. A different approach was taken by *Morzfeld et al.* [2017], who assimilated paleomagnetic data into several low-

degree dynamical models. They demonstrated skill in forecasting reversals 4 kyr into the future and concluded that a reversal in the next few kyr was unlikely. Extending these predictions in time was limited by the use of dynamical models in which one or more of the state variables were not directly constrained by observations. Uncertainties in the unobserved states were found to adversely affect the reliability of the predictions. In this study we extend the time frame for predictions by using several compilations of paleomagnetic observations to construct a stochastic model for fluctuations in the dipole field. Once the stochastic model is established, well-known methods offer a rigorous assessment of the reversal probability for arbitrary times into the future. It is important to point out that these predictions are inherently statistical in that we cannot forecast the outcome of a single realization. Instead, we predict the probability of ending up with a magnetic field in the opposite polarity after a specified period time.

Our predictions are contingent on the choice of stochastic model. This dependence might be perceived as a drawback, but an advantage of the approach is that the basic form of the stochastic model is largely determined by paleomagnetic observations [e.g. *Buffett et al.*, 2013; *Meduri and Wicht*, 2016]. More importantly, it is possible to incorporate different types of observations into these models to improve the statistical description of dipole fluctuations, including properties like the mean rate of geomagnetic reversals [*Gee and Kent*, 2015]. This means that stochastic models offer an extendable strategy for combining diverse observations into a single quantitative framework for making probabilistic assessments of the field behavior.

Our assessment of the reversal probability should be interpreted as the average or expected number of realizations that enter the reversed state after a specified time, although we do not explicitly restore to realizations to assess this probability. Instead, the problem is formulated in terms of the adjoint to the Fokker-Planck equation, which is sometimes called the backward Fokker-Planck equation. Numerical solutions of the backward Fokker-Planck equation yield simple and direct estimates for the probability of reversal. We proceed with a brief description of the stochastic model used in this study and outline the formulation of the backward Fokker-Planck equation. Quantitative estimates for the probability of reversal are given for the next few tens of thousands of years.

2. Stochastic Model for the Dipole Moment

Time variations in the axial dipole moment, $x(t)$, are governed by a stochastic differential equation [e.g. Van Kampen, 2007]

$$\frac{dx}{dt} = v(x) + \sqrt{D(x)}\,\Gamma(t) \tag{1}$$

where the drift term, $v(x)$, describes the deterministic evolution of the dipole moment and the noise term, $D(x)$, defines the amplitude of random variations. The time dependence of the random process, $\Gamma(t)$, is represented by uncorrelated Gaussian noise. The time average of $\Gamma(t)$ vanishes

$$< \Gamma(t) >= 0 \tag{2}$$

and the autocorrelation function is defined by a delta function

$$< \Gamma(t_1)\Gamma(t_2) >= 2\delta(t_1 - t_2)\,, \tag{3}$$

where the factor of two is a common convention. The idealization of the autocorrelation in terms of a delta function is intended to approximate a noise source with a short correlation time relative to the sampling of $x(t)$. Figure 1 shows estimates for the drift and noise terms recovered by *Buffett and Puranum* [2017] from stacks of relative paleointensity measurements from the past two million years [*Ziegler et al.*, 2011], supplemented with higher resolution measurements from the past 10 kyr [*Constable et al.*, 2016]. The noise term is approximated as a constant, while the drift term is defined by the extended model in equation (26) of *Buffett and Puranum* [2017]

The random component of the stochastic model in (1) introduces uncertainty into $x(t)$ as the solution evolves forward in time. The probability of $x(t)$ is commonly specified in terms of a transitional probability, $p(x,t|x',t')$, which describes the probability of the dipole moment evolving from x' at some initial time t' to x at some later time $t > t'$. When the initial state is also uncertain (denoted by $p(x',t')$), the probability of the subsequent state is

$$p(x,t) = \int p(x,t|x',t')p(x',t')\,dx'\,, \tag{4}$$

where we follow the usual custom of using $p(x,t)$ to define the probability density of x at time t. When the initial state is known (e.g. $p(x',t') = \delta(x'-x_0)$), the probability of $x(t)$ is given by

$$p(x,t) = \int p(x,t,|x',t')\delta(x'-x_0)dx' = p(x,t|x_0,t')\,. \tag{5}$$

In other words, the probability of the later state is equivalent to the transitional probability for a known initial state.

Both the transitional probability $p(x,t|x',t')$ and the more general expression for $p(x,t)$ from (4) evolve with time according to the Fokker-Planck equation [Risken, 1989]

$$\frac{\partial p}{\partial t} = \mathcal{L}\, p\,, \tag{6}$$

where

$$\mathcal{L} = \left(-\frac{\partial}{\partial x} v(x) + \frac{\partial^2}{\partial x^2} D(x) \right) . \tag{7}$$

Here the drift and noise terms are assumed to be independent of time, although this restriction is not essential. In many situations the Fokker-Planck equation provides a powerful tool for evaluating the probability of a stochastic process. We adopt this general approach here, although similar information can also be inferred from a large number of realizations of the stochastic model. We might use these realizations to evaluate the mean or variance at some later time. Both of these approaches are commonly used to characterize the statistics of the later state, given a description of the initial state.

The problem of determining the likelihood of a future polarity reversal is different because we know the end state (e.g. the dipole moment has reversed) and we seek to determine the probability of that event given a particular starting condition. For present purposes we denote the reversed state by $x(t) < 0$ and refer to this subset of states as the target set. The machinery needed to estimate probability of entering the target set is based on the adjoint equation to the Fokker-Planck equation, which is often called the backward Fokker-Planck equation [*Gardiner*, 2002].

3. Application of the Adjoint Equation

The adjoint equation is used to quantify the probability of $x(t)$ being in the target set (e.g. $x < 0$), subject to the condition that the dipole moment starts in a prescribed initial state x' at time t'. We define a function, $f(x)$, to specify whether $x(t)$ is in the target set. We let $f(x) = 1$ when $x < 0$ and set $f(x) = 0$ otherwise. The probability that $x(t)$ ends in the target state at time t is given by

$$u(x', t') = \int f(x) p(x, t|x', t')\, dx\,, \tag{8}$$

which is equivalent to the expected value of $f(x)$ once $x(t)$ is evolved from the initial state x' at t'. Any given realization for $x(t)$ will give either 0 or 1 for the value of $f(x)$, but the average (or expected) value defines the probability. The future time t of the reversed state is specified, so the probability u depends solely on x' and t'. An equivalent estimate of the expected value could also be obtained from realizations of the stochastic model: each realization is started at the initial condition $x(t') = x'$ and the mean value of $f(x)$ would be computed from the ensemble of solutions at t. When $t' \to t$ and $p(x, t|x', t') \to \delta(x - x')$ in (8), we find that

$$u(x', t) = f(x') \tag{9}$$

which serves as an *initial* condition when the evolution of $u(x', t')$ is integrated backward in time from $t' = t$, the final state of the system.

The time derivative of $u(x', t')$ for backward integration is defined by

$$-\frac{\partial u(x', t')}{\partial t'} = -\int f(x)\, \frac{\partial}{\partial t'}\, p(x, t, |x', t')\, dx \tag{10}$$

where the change in the transition probability is taken with respect to the initial time t' rather than the final time t (compare with the Fokker-Planck equation in (6)). The required derivative of the transition probability is defined by the backward Fokker-Planck equation [*Gardiner*, 2002]

$$-\frac{\partial p(x,t|x',t')}{\partial t'} = \mathcal{L}^\dagger p(x,t|x',t') \tag{11}$$

where

$$\mathcal{L}^\dagger = \left(v(x')\frac{\partial}{\partial x'} + D(x')\frac{\partial^2}{\partial x'^2} \right) \tag{12}$$

is the adjoint operator of $\mathcal{L}$ in (7), subject to the condition $p \to 0$ as $x \to \pm\infty$. Substituting (11) into (10) and interchanging the order of differentiation and integration gives

$$-\frac{\partial u(x',t')}{\partial t'} = \mathcal{L}^\dagger \int f(x) p(x,t|x',t')\, dx = \mathcal{L}^\dagger u(x',t')\,. \tag{13}$$

We use (13) to integrate $u(x',t')$ backward in time using (9) as an initial condition. Reflecting boundary conditions

$$D(x')\frac{\partial u}{\partial x'} = 0 \tag{14}$$

are adopted at the upper and lower limits of the domain in x'. If we view the calculation as the outcome of an infinite number of realizations then the boundary condition are equivalent to ensuring that no realizations leave the domain. We also adopt a sufficiently broad domain ($|x| < 12 \times 10^{22}$ Am^2) so that the probability of reaching the upper or lower limits is effectively zero. Additional calculations confirm that an increase the size of the domain does not change the result. In summary, numerical solutions of (13) are used to predict the probability of a reversed field at t, given the magnitude and sign of the dipole field at t'.

4. Probability of the Next Polarity Reversal

Figure 2 shows solutions for $u(x', t')$ at two time differences $\tau = t - t' = 10$ kyr and 20 kyr. When the initial state, x', is already inside the target set, it is quite likely that the dipole remains in the reversed state at 10 kyr and 20 kyr. There is a much smaller probability for a field with a positive initial polarity to reverse after 10 or 20 kyr. The details depend on the amplitude of the dipole at t', and there is a general trend for $u(x', t')$ to decrease at larger values for the initial field. For the present-day axial dipole moment, $x' = 7.6 \times 10^{22}$ A m^2 [*Gillet et al.*, 2013], a reversal is expected to occur after 20 kyr with a probability of 0.019. Longer integrations of $u(x', t')$ for larger time differences τ eventually yield a constant probability of 0.5 for all values of x'. This is expected as the probability of finding the field in the reversed state at some distant time in the future is 50%, independent of the initial amplitude of the dipole moment, subject to the assumption that the field spends equal time in both polarities. (This assumption is implicit in the construction of the stochastic model because the drift term is required to be an odd function of x.)

Shorter time integrations offer more meaningful insights. Figure 3 shows a prediction for the probability of reversal as a function of the time difference τ when $x' = 7.6 \times 10^{22}$ A m^2. Initially, the chance of reversal is very low because the noise term is unable to drive the dipole moment into the opposite polarity over a few thousand years. The root-mean-square change in the dipole moment due solely to noise is

$$< \Delta x^2 >^{1/2} = \sqrt{2D\Delta t}\,. \tag{15}$$

The expected change (or standard deviation) after 20 kyr is roughly 3.7×10^{22} A m^2 using $D = 340 \times 10^{44}$ A^2 m^4 Myr^{-1} [*Buffett and Puranum*, 2017]. This change in $x(t)$ is less than half the distance to the origin $x = 0$, so the noise term is not expected to drive the solution to the point of reversal after 20 kyr. Larger changes are possible, but these are less likely. For example, the change in dipole moment required to reach the onset of reversal ($x = 0$) is slightly in excess of two standard deviations. Consequently, we require an unusual sequence of events to move the present-day dipole moment to zero. A steady increase in probability $u(x', t')$ occurs once τ exceeds 15 kyr, although the predicted probability only reaches 11% after 50 kyr. Thus the prospects of an imminent geomagnetic reversal is low given the paleomagnetic record from PADM2M and CALS10k.2.

5. Discussion

The stochastic model offers a useful perspective for interpreting the recent historical decline in the dipole field. Over a 150-year interval between 1860 and 2010 the dipole moment has decreased by $\Delta x = 0.68 \times 10^{22}$ A m^2 [*Gillet et al.*, 2013], compared with the standard deviation $< \Delta x^2 >^{1/2} = 0.32 \times 10^{22}$ A m^2 from (15). Consequently, the observed change exceeds the standard deviation by a factor of 2.13, corresponding to a probability of 1.7% for Gaussian distributed noise. While the recent historical decline is unusual, it is within the allowable variation of the model. Extending the current linear trend over the next 1700 years would bring the dipole moment to zero (i.e. $\Delta x = 7.6 \times 10^{22}$ A m^2), whereas the standard deviation for this time interval is only $< \Delta x^2 >^{1/2} = 1.08 \times 10^{22}$ A m^2. Changing $x(t)$ by seven times the standard deviation is highly unlikely, and this assessment is overly optimistic. A full description of the dipole evolution includes the drift

term, which is positive once $x(t)$ drops below the time-averaged dipole ($< x >= 5.3 \times 10^{22}$ A m^2). A positive drift opposes the steady decline and makes the prospect of a reversal in the next 1700 years even more unlikely. By comparison, the drift would contribute to the recent historical trend because we expect a negative drift with the current dipole moment (see Fig. 1).

Another point of reference for appraising our prediction is obtained by assuming that reversals obey a Poisson process [*Cox*, 1969]. Such a process lacks memory, so the cumulative probability of a reversal within a specified time interval, Δt, is independent of the prior history. Instead, the probability is specified by the mean reversal rate, which is approximately $r = 4.4$ Myr^{-1} over the past 5 Myr [*Ogg*, 2012]. The cumulative probability of a reversal occurring within the time interval Δt is given by

$$P(t < \Delta t) = 1 - e^{-r\Delta t} \tag{16}$$

which yields $P = 0.084$ for $\Delta t = 20$ kyr. By comparison, the prediction from our stochastic model ($P = 0.019$) is much lower because the noise term limits the rate at which the dipole approaches a reversed state. Extending the time interval to $\Delta t = 50$ kyr, increases the reversal probability for the Poisson process to 0.197. A similar increase in probability ($P = 0.11$) is predicted using the stochastic model. These two estimates have been brought into slightly closer agreement, which can be interpreted as greater agreement in the underlying assumptions. A larger value for Δt lowers the dependence of the stochastic model on initial conditions, which makes the statistical description more like a process with no memory. However, our predictions over the next 10^4 years are still strongly

dependent on the initial state. On the other hand, there is no dependence on the current rate of change in the dipole.

Strictly speaking, the cumulative probability for a Poisson process differs conceptually from the prediction of the backwards Fokker-Planck equation. In former case we predict the probability of a chron duration and in the latter we predict the probability of ending up in the reversed state. For very large Δt the Poisson process predicts $P \to 1$, whereas the probability of being in the reversed state is $P \to 0.5$. In principle, a realization can enter the reversed state and subsequently revert back to the normal state by the end of the prescribed time interval. Such a path would be recorded as a realization in the normal state (e.g. not in the target set). However, the probability of this event is greatly reduced at short Δt because the actual reversal would need to occur within a shorter time frame. As long as the probability of this earlier event is low, it should not affect our interpretion reversal probabilities.

6. Concluding Remarks

Quantitative predictions for the probability of reversal are dependent on the underlying stochastic model. The stochastic model used here is constructed from two compilations of paleomagnetic measurements. The noise term is inferred from the high-resolution CALS10k.2 model [*Constable et al.*, 2016], and the drift term is recovered from the longer PADM2M model [*Ziegler et al.*, 2011]. It is encouraging that our stochastic model also gives reasonable predictions for the mean reversal rate ($r = 4.2$ Myr^{-1}), as well as the duration of polarity transitions [*Buffett and Puranum*, 2017], even though this information was not used in constructing the model. This consistency lends support to the model.

On the other hand, the model is not capable of reproducing systematic features prior to a reversal [e.g *Valet et al.*, 2012] because the evolution of the dipole into a reversal is driven by random noise. Extensions of the model are required to account for any recurrent behavior prior to a reversal. Other sources of information could also be incorporated into the model to improve the predictions. A notable example is the evidence for asymmetry in the growth and decay of the geomagnetic dipole [*Avery et al.*, 2017], which could be related to the shape of the drift term. In summary, the stochastic model provides a framework for combining a variety of paleomagnetic observations into a quantitative statistical description of the field behavior. Current estimates of the stochastic model suggest that the next geomagnetic reversal is improbable in the next 10 to 20 kyr.

Acknowledgments. This work is partially supported by the National Science Foundation (EAR-1644644). We thank Phil Livermore and Matti Morzfeld for thoughtful comments and suggestions, which improved the paper. All software used to generate the results in this paper are included in an electronic supplement.

References

Aubert, J. (2014). Earth's core internal dynamics 1840-2000 imaged by inverse dynamo modelling, *Geophys. J. Int.*, *197*, 119-134.

Aubert, J. and A. Fournier (2011). Inferring internal properties of Earth's core dynamics and their evolution from surface observations and a numerical geodynamo model, *Nonlin. Processes Geophys.*, *18*, 657-674.

Avery, M., J.S. Gee and C.G. Constable (2017) Asymmetry in growth and decay of the geomagnetic dipole revealed in seafloor magnetization, *Earth Planet. Sci. Lett.*, *467*, 79-88.

Buffett, B., L. Ziegler and C.G. Constable (2013). A stochastic model for palaeomagnetic field variations, *Geophys. J. Int.*, *195*, 86-97.

Buffett, B. and A. Puranum (2017). Constructing stochastic models for dipole fluctuations from paleomagnetic observations, *Phys. Earth Planet. Inter.*, *272*, 68-77.

Cox, A. (1969), Geomagnetic reversals, *Science*, *163*, 237-245.

Constable, C. and M. Korte (2004). Is Earth's magnetic field reversing? *Earth Planet. Sci. Lett.*, *246*, 1-16.

Constable, C., M. Korte and S. Panovska (2016). Persistent high paleosecular variation activity in southern hemisphere for at least 10,000 years, The complexity of reversals, *Earth Planet. Sci. Lett.*, *453*, 78-86.

Davidson, P.A. (2016). *An Introduction to Magnetohydrodynamics*, Cambridge University Press, Cambridge.

Finlay, C.C., J. Aubert and N. Gillet (2016). Gyre-driven decay of the Earth's dipole, *Nature Comm.*, *7*, 10422.

Gardiner, C.W. (2002). *Handbook of Stochastic Methods for Physics, Chemistry and the Natural Sciences*, 2nd Edition, Springer, New York.

Gee, J.S. and D.V. Kent (2015). Sources of oceanic magnetic anomalies and the geomagnetic polarity timescale, in *Treatise on Geophysics*, 2nd Edition, ed. G. Schubert, *5*, 419-460.

Gillet, N., D. Jault, C.C. Finlay and N. Olsen (2013). Stochastic modeling of the Earth's magnetic field: Inversion for covariances over the observatory era, *Geochem. Geophys. Geosys.*, *14*, 766-786.

Gillet, N., D. Jault and C.C. Finlay (2015). Planetary gyre, time-dependent eddies torsional waves, and equatorial jets at the Earth's core surface, *J. Geophys. Res.*, *120*, 3991-4013.

Hulot, G., C. Eymin, B. Langlais, M. Miorari and N. Olsen (2002). Small-scale structure of the geodynamo inferred from Oersted and Magsat, *Nature*, *416*, 620-623..

Hulot, G., F. Lhuillier, and J. Aubert (2010). Earth's dynamo limit of predictability, *Geophys Res. Lett.*, *37*, L06305.

Kuang, W., A. Tangborn, Z. Wei and T. Sabaka (2009). Constraining a numerical geodynamo model with 100 years of surface observations, *Geophys. J. Int.*, *179*, 1458-1468.

Malin, S.R.C. (1996). Historical introduction to geomagnetism, in *Geomagnetism*, *vol. 1*, Academic Press, London, 1-49.

Metman, M.C., P.W. Livermore, and J.E. Mound (2018). The reversed and normal flux contributions to axial dipole decay for 1880-2015, *Phys. Earth Planet. Inter.*, *in press.*

Morzfeld, M., A. Fournier and G. Hulot (2017). Coarse predictions of dipole reversals by low-dimensional modeling and data assimilation, *Phys. Earth Planet. Inter.*, *262*, 8-17.

Meduri, D.G. and J. Wicht (2016). A simple stochastic model for dipole fluctuations in numerical dynamo models, *Front. Earth Sys.*, *4:38*, doi: 10.3389/feart2016.00038.

Ogg, J.G. (2012), Geomagnetic polarity time scale, in *The Geological Time Scale 2012*, ed. F.M. Gradstein et al., Elsevier Science, Chap. 5, 85-113.

234 Olson, P.L. (2002). Geophysics: The disappearing dipole, *Nature*, *416*, 591-593.

235 Olson, P.L., G.A. Glatzmaier, G.A. and R.S. Coe (2011). Complex polarity reversals in a
236 geodynamo model, *Earth Planet. Sci. Lett.*, *304*, 168-179.

237 Risken, H., (1989). *The Fokker-Planck Equation*, Springer, New York.

238 Poletti, W., A.J. Biggin, R.I.F. Trindale, G.A. Hartmann, and F. Terra-Nova (2018).
239 Continuous millenial decrease of the Earth's magnetic axial dipole, *Phys. Earth Planet.*
240 *Inter.*, *274*, 72-86.

241 Valet, J.P., A. Fournier, V. Courtillot, and E. Herrero-Bevera (2012). Dynamical similarity
242 of geomagnetic field reversals, *Nature*, *490*, 89-93.

243 Van Kampen, N.G., *Stochastic Methods in Physics and Chemistry*, North-Holland, Ams-
244 terdam.

245 Ziegler, L.B., C.G. Constable, C.L. Johnson, and L. Tauxe (2011). PADM2M: A penalized
246 maximum likelihood model of the 0-2 Ma palaeomagnetic axial dipole moment, *Geophys.*
247 *J. Int.*, *184*, 1069-1089.

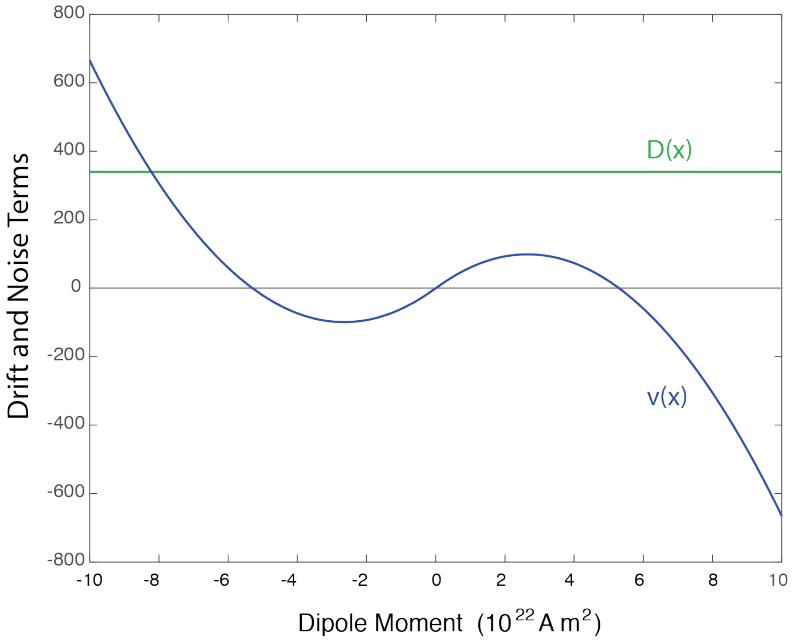

Figure 1. Drift, $v(x)$, and noise, $D(x)$, terms recovered from paleomagnetic observations (see text). The units of $v(x)$ and $D(x)$ are 10^{22} $\mathrm{Am^2Myr^{-1}}$ and 10^{44} $\mathrm{A^2m^4Myr^{-1}}$, respectively.

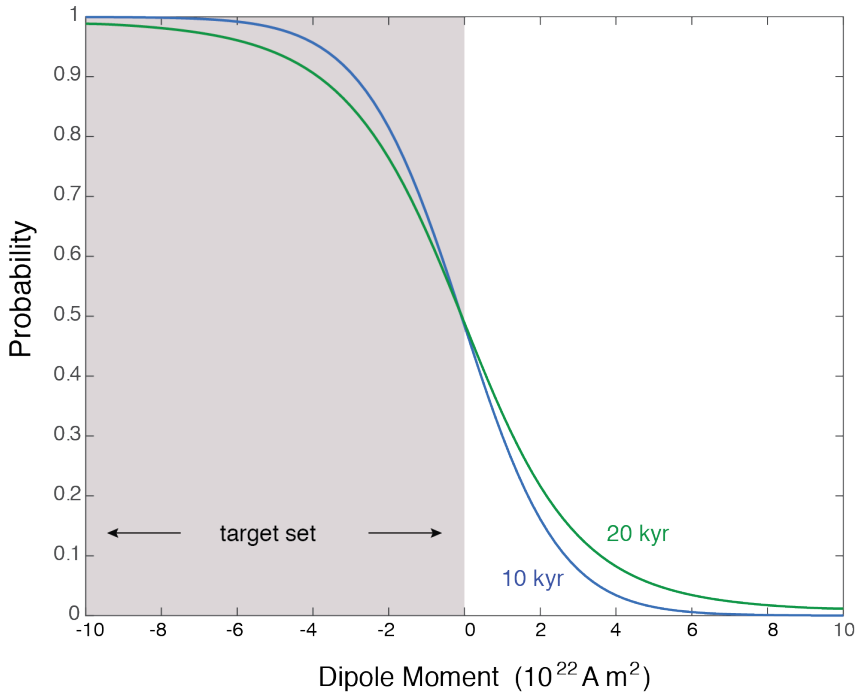

Figure 2. Reversal probability, $u(x', t')$, as a function of x' for two different values of the time difference $\tau = t - t'$. The probability of moving from positive x' to the reversed state $x < 0$ increases with larger time differences.

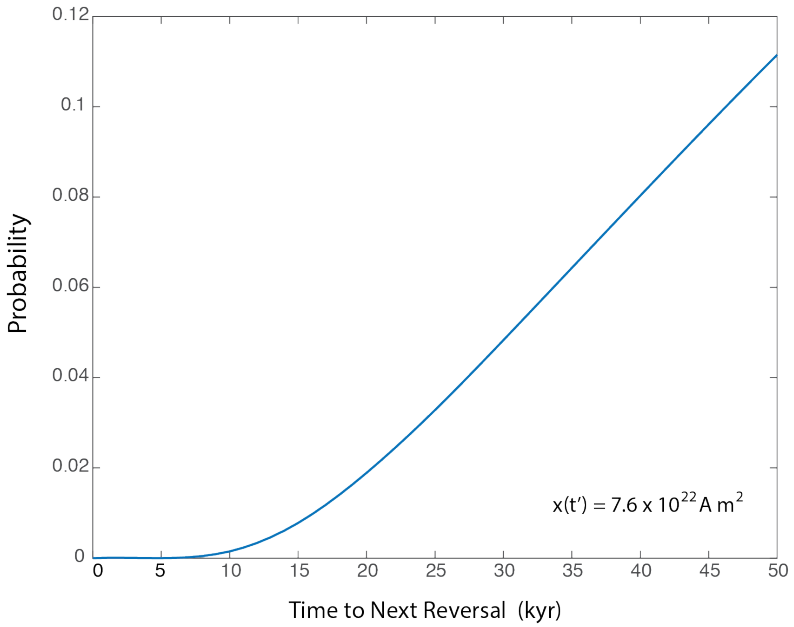

Figure 3. Reversal probability as a function of time difference $\tau = t - t'$ for an initial dipole moment of $x' = 7.6 \times 10^{22}$ A m^2. The time difference can be interpreted as the time to the next reversal from the present-day state. The predicted probability is low during the first 10 kyr, but increases linearly with τ after 15 kyr and reaches 11% after 50 kyr.